Middle-East Journal of Scientific Research 22 (9): 1422-1429, 2014
ISSN 1990-9233

DOI: 10.5829/idosi.mejsr.2014.22.09.22064

Estimation of the Flow and Heat Transfer in MHD Flow of a Power Law Fluid over a Porous Plate Using Artificial Neural Networks

M. Farahi Shahri and A. Hossein Nezhad

Department of Mechanical Engineering,
University of Sistan and Baluchestan, Zahedan 98135-987, Iran

Abstract: In this study, the prediction of the flow and heat transfer from a porous plate subjected to the MHD flow of a power law fluid is investigated using artificial neural networks (ANNs). A numerical study is performed to estimate the flow and heat transfer characteristics as a function of some input parameters, namely power law index, injection or suction speed, magnetic parameter and Eckert number. The governing equations along with the appropriate boundary conditions are transformed into two boundary value problems (BVPs) of third and second orders ordinary differential equations and are solved via Keller–Box method and then the ANN is applied to them. Back-Error Propagation (BEP) neural network is used for predicting the desired outputs. Results of the numerical data and the ANN are in good agreements with errors less than 5%. According to findings of this paper, the ANNs could be used efficiently for simulating of heat transfer in MHD flow of a power law fluid over a porous plate.

Key words: Power law fluid · Magnetohydrodynamics · Similarity solution · Artificial neural network

INTRODUCTION

The problem of a non-Newtonian fluid passing a porous plate under the influence of a magnetic field has attracted the interest of different research communities because of its various applications. In view of these applications, Sarpakaya [1] was the first among others to examine the magnetohydrodynamic (MHD) flow of non-Newtonian fluids. Later this work was extended by many authors by considering the non-Newtonian viscoelastic flow, heat and mass transfer under different physical situations [2-5]. The most common type of time-independent non-Newtonian fluid behavior observed is shear-thinning (pseudoplasticity), characterized by an apparent viscosity which decreases with increasing shear rates [6]. Another type of fluid behavior is shear-thickening (dilatants) in that the apparent viscosity increases with increasing shear rate [6]. These two behaviors may be represented by the power-law model, the simplest and the most widely used model in the literature [7].

The MHD flow problems of power law fluids are intrinsically nonlinear like the most fluid mechanics problems and do not have an exact solution. However, numerical solution for these kinds of problems has been widely reported in the literature [8-10]. A few recent publications in which the MHD flow problems of power law fluids are addressed can be seen in [11]. All techniques available in the literature for these problems are based on well known deterministic numerical procedures; there is a need therefore to explore stochastic numerical methods based on computational intelligence techniques to solve these problems [12]. Stochastic solvers based on artificial neural networks have been examined widely by the researchers to solve a variety of linear and non-linear differential equations [13-15]. A few recent applications of these solvers are heat transfer in corrugated channels [16], prediction of the performance of heat exchangers in newly designed refrigerators [17], evaluation of surface heat transfer coefficient at the liquid–solid interface [18], solar water heating systems [19], Exergy analysis of an ejector-absorption heat transformer [20], simulating of dehumidifiers [21, 22], optimization of entropy generation in unsteady MHD flows [23] and etc.

The literature review reveals that the ANNs have been quite promising in offering solutions to non-linear problems. The ANN method has not been used or tested

Corresponding Author: M. Farahi Shahri, Department of Mechanical Engineering, University of Sistan and Baluchestan, Zahedan 98135-987, Iran.

for heat transfer analysis of MHD flow of power law fluids. Therefore, this study primarily focuses on the applicability of the ANN method for the heat transfer analysis MHD flow of a power law fluid over a porous plate. In the present study, the effects of effective parameters on the flow and heat transfer characteristics are investigated and the numerical results are presented in comparison with the results of ANN method.

The organization of the paper is as follows. In Section 2, a flow analysis is performed and required transformed equations and boundary conditions are presented. Like this in Section 3, a heat transfer analysis is performed and the transformed energy equation and boundary conditions are presented. In Section 4, the appropriate ANN is applied to the problem and training procedure for the ANN is presented; a Back-Error Propagation (BEP) training algorithm is employed to train the network and find the best weights and the performance of the ANN is examined. In the last section, the achievements of this study are concluded along with some trends for future works.

Flow Analysis: Consider a viscous, steady two-dimensional flow of an incompressible, electrically conducting power law fluid in the presence of a transverse magnetic field over a stretching plate. The thermo-physical properties of the plate and the fluid are assumed to be constant. The flow is affected by an external transverse uniform magnetic field $B \equiv (0, B_0, 0)$. The magnetic Reynolds number is considered to be small so that the induced magnetic field is negligible. Under these assumptions, the governing equations are given by

$$\frac{\partial u}{\partial x}+\frac{\partial v}{\partial y}=0 \tag{1}$$

$$u\frac{\partial u}{\partial x}+v\frac{\partial u}{\partial y}=-\frac{K}{\rho}\frac{\partial}{\partial y}\left(-\frac{\partial u}{\partial y}\right)^{n}-\frac{\sigma B_0^2}{\rho}u \tag{2}$$

where K is the consistency index of the fluid and n is the Power-Law index according to which shear-thinning or shear-thickening behavior is regarded for n □ 1 or n □ 1, respectively [24]. The suitable boundary conditions are as follows:

$$u(x,0)=U, \tag{3}$$

$$v(x,0)=v_W, \tag{4}$$

$$u\to 0 \quad \text{as} \quad y\to\infty \tag{5}$$

where v_w is the suction velocity if $v_w < 0$ and it is blowing velocity if $v_w > 0$. The following similarity transformations are employed to convert the governing equations into ordinary differential equations:

$$\eta=\frac{y}{x}(Re_x)^{\frac{1}{n+1}}, \quad \psi(x,y)=bx^2(Re_x)^{\frac{-1}{n+1}}f(\eta) \tag{6}$$

where η is the similarity variable and ι (x, y) is the stream function. The local Reynolds number and the magnetic parameter are defined as:

$$Re_x=\frac{U^{2-n}x^n}{\upsilon} \tag{7}$$

$$Mn=\frac{\sigma B_0^2}{\rho b} \tag{8}$$

The conservation of mass is therefore automatically satisfied and the momentum equation and the corresponding boundary conditions can be considered as

$$n\left(-f_{\eta\eta}\right)^{n-1}f_{\eta\eta\eta}-f_\eta^2+\left(\frac{2n}{n+1}\right)ff_{\eta\eta}-Mnf_\eta=0 \tag{9}$$

$$f_\eta(0)=1, \tag{10}$$

$$f(0)=R, \tag{11}$$

$$f_\eta(\eta)\to 0 \quad \text{as} \quad \eta\to\infty \tag{12}$$

The subscript η denotes differentiation with respect to η. Although the transformation defined in (7) results in a proper similarity problem only if U varies with x^m. Here m is an arbitrary positive constant (not essentially an integer). In the conditions (11) injection or suction velocity v_W should be rewritten as

$$R=-\frac{n+1}{2n}\left(\frac{(Re_x)^{\frac{1}{(n+1)}}}{U}\right)v_W \tag{13}$$

Therefore, R is introduced to signify the surface mass transfer which is positive for blowing and negative for suction. The skin friction coefficient at the plate is given by

$$C_f=2(Re_x)^{\frac{-1}{n+1}}\left[-f_{\eta\eta}(0)\right]^n \tag{14}$$

To assess the heat transfer characteristics of the problem, the energy equation is solved in the next section.

Heat Transfer Analysis: The general energy equation is given by

$$\rho c_P\left(u\frac{\partial T}{\partial x}+v\frac{\partial T}{\partial y}\right)=\frac{\partial}{\partial y}\left(\alpha\frac{\partial T}{\partial y}\right)+\mu\left(\frac{\partial u}{\partial y}\right)^{n+1}+\sigma B_0^2u^2 \tag{15}$$

where c_p is the specific heat at constant pressure, T is the fluid temperature and α is the thermal conductivity of the fluid. The second and third terms on the right-hand side of (14) represent the viscous dissipation and the Ohm heating parameter, respectively. The appropriate boundary conditions are

$$T=T_W=T_\infty+A\left(\frac{x}{\ell}\right)^2 \quad \text{at} \quad y=0$$
$$T\to T_\infty \quad \text{as} \quad y\to\infty \tag{16}$$

where T_∞ is the free stream temperature, T_w is the wall temperature and A is a constant, which depends on the properties of the fluid and l is a characteristic length. In terms of the dimensionless below quantities,

$$\theta=\frac{T-T_\infty}{T_W-T_\infty} \quad \text{where} \quad T_W-T_\infty=A\left(\frac{x}{\ell}\right)^2 \tag{17}$$

The energy equation (18) converts to the following equation:

$$\theta_{\eta\eta}+\Pr\left(\frac{2n}{n+1}f\theta_\eta-2f_\eta\theta\right)=\Pr Ec\left\{\left(f_{\eta\eta}\right)^{n+1}+Mnf_\eta^2\right\} \tag{18}$$

Boundary conditions are given by

$$\theta(\eta)=1 \quad \text{at} \quad \eta=0, \quad \theta(\eta)\to 0 \quad \text{as} \quad \eta\to\infty \tag{19}$$

The parameters Pr and Ec are the modified Prandtl number and Eckert number, respectively and are as

$$\Pr=\frac{\rho c_P b x^2}{\alpha}\left(Re_x\right)^{\frac{-2}{n+1}}, \quad Ec=\frac{\upsilon l^2 b^n}{c_P A x^2}Re_x \tag{20}$$

The local Nusselt number is given by

$$Nu_x=-Re_x^{\frac{1}{n+1}}\theta'(0) \tag{21}$$

Artificial Neural Networks: Artificial neural networks (ANNs) consisting of very simple and extremely interconnected processors called neuron are commonly used in biological studies because they are believed to be universal approximates of any continuous function. As shown in Fig. 1, the neurons are connected to each other by weighted links that knowledge is stored in them. Each neuron receives multiple inputs from other neurons in proportion to their connection weights and generates a single output which may be propagated to several other neurons [18].

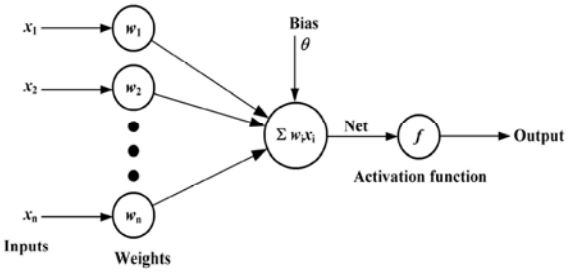

Fig. 1: An artificial neuron structure.

Among many types of ANNs, the most extensively used is the feed-forward neural network such as multilayer perceptron (MLP) network with Back-Error Propagation (BEP) training algorithm. The MLP consists of at least three or more layers, which comprises an input layer, an output layer and a number of hidden layers. Each neuron in one layer is connected to the neurons in the next layer and there are no connections among the units of the same layer [25, 26]. The number of neurons in each layer may be different depending on the problem.

The weighted sum of input components is calculated as [27]:

$$Net_j=\sum_{i=1}^{p}w_{ij}x_i+\theta_j \tag{22}$$

where Net_j is the weighted sum of the jth neuron for the input received from the preceding layer with p neurons, w_{ij} is the weight between the jth neuron and the ith neuron in the preceding layer, x_i is the output of the ith neuron in the preceding layer, θ_j is the bias term of the jth neuron. The output of the jth neuron (out_j) is calculated with a logistic sigmoid (logsig) function as follows:

$$out_j=f\left(Net_j\right)=\frac{1}{1+e^{-Net_j}} \tag{23}$$

The training of the network is accomplished by adjusting the weights and is carried out through a large number of training sets and training cycles (epochs). The purpose of the learning procedure is to find the optimal set of weights, which in an ideal case would produce the

correct output for any relative input. The output of the network is compared with a desired response to determine an error. The performance of the MLP is measured in terms of a desired signal and the criterion for convergence. For one sample, the root mean square error (RMSE) and the absolute fraction of variance (R^2) are determined from

$$\mathrm{RMSE} = \sqrt{\frac{1}{M}\sum_{i=1}^{M}(T_i - out_i)^2} \tag{24}$$

$$R^2 = 1 - \frac{\sum_{i=1}^{M}(T_i - out_i)^2}{\sum_{i=1}^{M}(T_i)^2} \tag{25}$$

where T_i and out_i are the desired (target) output and output of neural network values respectively for the ith output neuron and M is total number of data sets. The absolute fraction of variance ranges between 0 and 1. The values closer to 1 indicate a very good fit, while the values closer to 0 indicate a poor fit [28].

In this study, ANN structure has been designed and trained using the MATLAB Neural Network Toolbox. The Back-Error Propagation (BEP) training algorithm has been used in feed-forward with one hidden-layer. As shown in Fig. 2, in the structural network the inputs are the power law index (n), injection or suction speed (v_w), magnetic parameter (Mn) and Eckert number (Ec) and the outputs are the skin friction (C_f) and Nusselt number (Nu).

A sigmoid function has been used as the activation function of artificial neurons and training has been done using a fixed (4000) number of epochs. The total 30 numerical results were used to train and test the ANN model for skin friction. The 8 data set were used for the training set and the rest of the data were used for testing the results of the model. The performance of skin friction (C_f) training and test sets of the proposed ANN model is shown in Figs. 3, 4 respectively.

The performance of training and test sets were given based on RMSE and R^2. As shown in the mentioned figures, the RMSE values of the model for training and test sets were 0.01559 and 0.02776 respectively. Like this the R^2 values of the model for training and test sets were 0.9973 and 0.9712 respectively. It is found that the ANN was properly trained, as it simulates complicated relationship between the input and output variables.

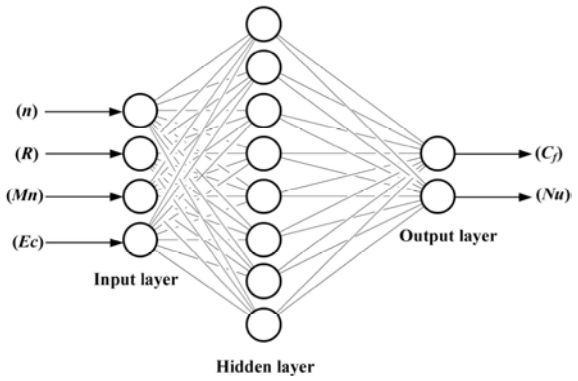

Fig. 2: Schematic diagram of a multi-layer ANN.

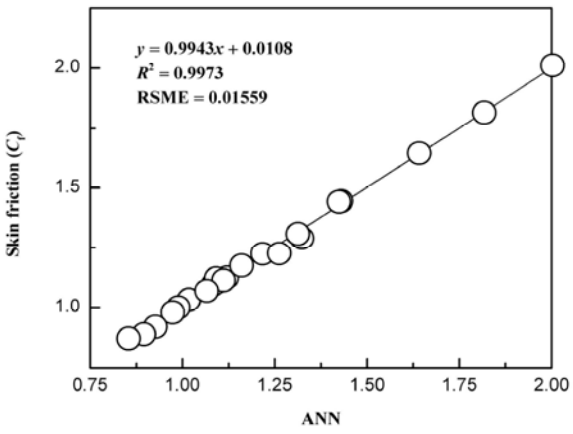

Fig. 3: Scatter plots of the training set for skin friction

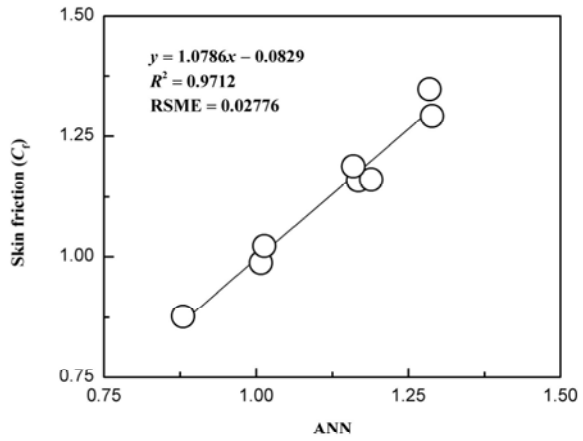

Fig. 4: Scatter plots of the testing set for skin friction

Calculated skin frictions from the ANN model for training and test sets and numerically obtained skin frictions are compared with and given in Table 1. As seen in Table 1 the maximum error is 4.678% in Exp-6 (in testing) and minimum error is 0.1337% in Exp-26 (in training). The results obtained from the ANN model are in good agreement with the numerical results within 5%

Table 1: Skin friction data for testing (bold data) and training (non-bold data) of the network.

	Input parameters					
Experiment	n	R	Mn	Numerical C_f	ANN C_f	Error (%)
Exp-1	0.4	-0.235	0.0	1.4451	1.4299	1.0500
Exp-2	0.4	-0.235	0.5	2.0103	2.0024	0.3923
Exp-3	0.8	-0.235	0.0	1.1588	1.1674	-0.7401
Exp-4	0.8	-0.235	0.5	1.4424	1.4239	1.2801
Exp-5	1.0	-0.235	0.0	1.1246	1.1204	0.3756
Exp-6	1.0	-0.235	0.5	1.3479	1.2847	4.6870
Exp-7	1.2	-0.235	0.0	1.1089	1.0993	0.8579
Exp-8	1.2	-0.235	0.5	1.2902	1.3234	-2.5694
Exp-9	1.6	-0.235	0.0	1.0934	1.0826	0.9813
Exp-10	1.6	-0.235	0.5	1.2239	1.2168	0.5800
Exp-11	0.4	0.0	0.0	1.2919	1.2891	0.2203
Exp-12	0.4	0.0	0.5	1.8151	1.8176	-0.1378
Exp-13	0.8	0.0	0.0	1.0315	1.0175	1.3640
Exp-14	0.8	0.0	0.5	1.3082	1.3128	-0.3512
Exp-15	1.0	0.0	0.0	1.0003	0.9888	1.1476
Exp-16	1.0	0.0	0.5	1.2248	1.2623	-3.0649
Exp-17	1.2	0.0	0.0	0.9874	1.0076	-2.0510
Exp-18	1.2	0.0	0.5	1.1750	1.1602	1.2622
Exp-19	1.6	0.0	0.0	0.9798	0.9735	0.6446
Exp-20	1.6	0.0	0.5	1.1207	1.0909	2.6548
Exp-21	0.4	0.235	0.0	1.1606	1.1887	-2.4262
Exp-22	0.4	0.235	0.5	1.6449	1.6415	0.2078
Exp-23	0.8	0.235	0.0	0.9200	0.9268	-0.7400
Exp-24	0.8	0.235	0.5	1.1879	1.1595	2.3859
Exp-25	1.0	0.235	0.0	0.8898	0.8958	-0.6795
Exp-26	1.0	0.235	0.5	1.1129	1.1114	0.1337
Exp-27	1.2	0.235	0.0	0.8771	0.8798	-0.3067
Exp-28	1.2	0.235	0.5	1.0687	1.0658	0.2680
Exp-29	1.6	0.235	0.0	0.8719	0.8539	2.0672
Exp-30	1.6	0.235	0.5	1.0222	1.0133	0.8730

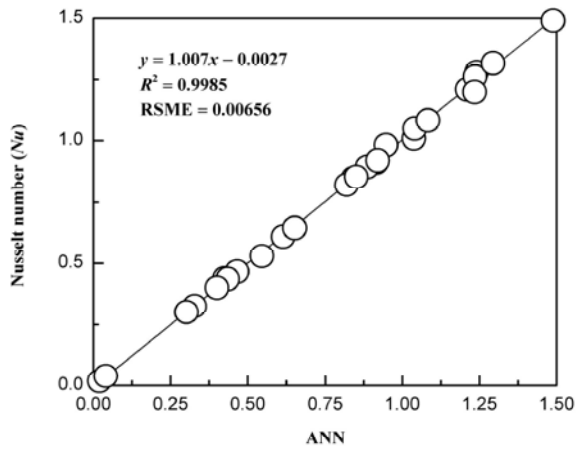

Fig. 5: Scatter plots of the training set for Nusselt number.

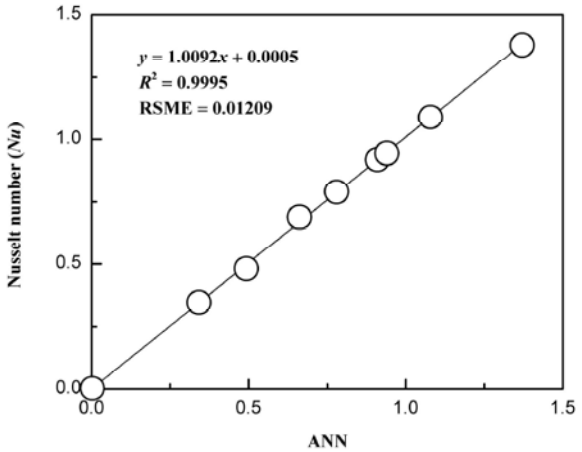

Fig. 6: Scatter plots of the testing set for Nusselt number.

confidence interval. This study so far reveals that skin friction can alternatively be modeled using the ANNs within a reasonable accuracy.

The Total 36 numerical results were used to train and test the ANN model for Nusselt number. The 9 data set were used for the training set and the rest of the data were used for testing the results of the model. The performance of training and test sets of the proposed ANN model is shown in Figs. 5, 6 respectively.

As shown in the figures, the RMSE values of the model for training and test sets were 0.00656 and 0.01209 respectively. Like this the R^2 values of the model for

Table 2: Nusselt number data for testing (bold data) and training (non-bold data) of the network.

	Input parameters						
					Numerical	ANN	
Experiment	n	R	Mn	Ec	Nu	Nu	Error (%)
Exp-1	0.4	-0.235	0.0	0	1.2092	1.2097	-0.045
Exp-2	0.4	-0.235	0.0	1	0.9133	0.9158	-0.276
Exp-3	0.4	-0.235	0.5	0	0.8491	0.8409	0.962
Exp-4	0.4	-0.235	0.5	1	0.3470	0.3423	1.346
Exp-5	1.0	-0.235	0.0	0	1.2793	1.2411	2.984
Exp-6	1.0	-0.235	0.0	1	1.0101	1.0371	-2.675
Exp-7	1.0	-0.235	0.5	0	0.9825	0.9476	3.556
Exp-8	1.0	-0.235	0.5	1	0.6101	0.6146	-0.744
Exp-9	1.6	-0.235	0.0	0	0.7894	0.7795	1.255
Exp-10	1.6	-0.235	0.0	1	0.4659	0.4659	-0.005
Exp-11	1.6	-0.235	0.5	0	0.4379	0.4242	3.126
Exp-12	1.6	-0.235	0.5	1	0.0024	0.0024	-0.845
Exp-13	0.4	0	0.0	0	1.2613	1.2363	1.984
Exp-14	0.4	0	0.0	1	0.9193	0.9095	1.065
Exp-15	0.4	0	0.5	0	0.8943	0.8862	0.907
Exp-16	0.4	0	0.5	1	0.3254	0.3279	-0.768
Exp-17	1.0	0	0.0	0	1.3799	1.3710	0.645
Exp-18	1.0	0	0.0	1	1.0501	1.0398	0.984
Exp-19	1.0	0	0.5	0	1.0835	1.0826	0.085
Exp-20	1.0	0	0.5	1	0.6452	0.6513	-0.951
Exp-21	1.6	0	0.0	0	0.8207	0.8198	0.105
Exp-22	1.6	0	0.0	1	0.4362	0.4346	0.356
Exp-23	1.6	0	0.5	0	0.4808	0.4927	-2.481
Exp-24	1.6	0	0.5	1	0.0188	0.0188	0.019
Exp-25	0.4	0.235	0.0	0	1.3160	1.2942	1.658
Exp-26	0.4	0.235	0.0	1	0.9209	0.9197	0.131
Exp-27	0.4	0.235	0.5	0	0.9450	0.9399	0.543
Exp-28	0.4	0.235	0.5	1	0.3008	0.3011	-0.094
Exp-29	1.0	0.235	0.0	0	1.4901	1.4890	0.077
Exp-30	1.0	0.235	0.0	1	1.0906	1.0785	1.109
Exp-31	1.0	0.235	0.5	0	1.1992	1.2349	-2.974
Exp-32	1.0	0.235	0.5	1	0.6883	0.6617	3.861
Exp-33	1.6	0.235	0.0	0	0.8546	0.8503	0.498
Exp-34	1.6	0.235	0.0	1	0.4010	0.4005	0.118
Exp-35	1.6	0.235	0.5	0	0.5297	0.5456	-2.995
Exp-36	1.6	0.235	0.5	1	0.0402	0.0401	0.178

training and test sets were 0.9985 and 0.9995 respectively. The highly closeness of R^2 values to unity shows that the proposed ANN model can predict the desired results properly for both training and test tests.

Calculated Nusselt numbers from the ANN model test sets and numerically obtained Nusselt numbers are compared with and presented in Table 2. As seen in Table 2 the maximum error is 3.861% in Exp-32 and minimum error is -0.005% in Exp-10. The results obtained from the ANN model are in good agreement with the numerical results within 5% confidence interval. In addition, this study reveals that the Nusselt number can alternatively be estimated using the ANNs within a reasonable accuracy, too. Thus according to the findings of present study, the proposed ANN model is altogether applied for MHD flow and heat transfer of a power law fluid over a porous plate, successfully.

CONCLUSION

In the current perusal, the ANN approach is developed successfully to simulate the heat transfer in MHD flow of a power law fluid over a porous plate. ANN structure has been trained and tested using the MATLAB environment. The results and comparative study indicate that the artificial neural network method is a suitable

method to estimate the heat transfer in MHD flow of a power law fluid over a porous plate. The prediction of the skin friction and the Nusselt number with the ANN model is in good agreement with the standard numerical data. The ANN model, which provides quick, exact and reliable results, is an efficient tool and useful alternative for the conventional time-consuming numerical methods. Also, one may extend this methodology to investigate other computational intelligence techniques based on the ANN models, such as heat transfer optimization of MHD flow of power law fluids with global and local search algorithms.

REFERENCES

1. Sarpkaya, T., 1961. Flow of non-Newtonian fluids in a magnetic field, AIChE Journal, 7(2): 324-328.
2. Abel, M.S. and N. Mahesha, 2008. Heat transfer in MHD viscoelastic fluid flow over a stretching sheet with variable thermal conductivity, non-uniform heat source and radiation, Applied Mathematical Modelling, 32(10): 1965-1983.
3. Chowdhury, M.K. and M.N. Islam, 2000. MHD free convection flow of visco-elastic fluid past an infinite vertical porous plate, Heat and Mass Transfer, 36(5): 439-447.
4. Khan, S., M.S. Abel and R. Sonth, 2003. Visco-elastic MHD flow, heat and mass transfer over a porous stretching sheet with dissipation of energy and stress work, Heat and Mass Transfer, 40(1-2): 47-57.
5. Abel, M.S. and M.M. Nandeppanavar, 2009. Heat transfer in MHD viscoelastic boundary layer flow over a stretching sheet with non-uniform heat source/sink, Communications in Nonlinear Science and Numerical Simulation, 14(5): 2120-2131.
6. Chhabra, R.P. and J.F. Richardson, 2008. Non-Newtonian flow and applied rheology engineering applications. Elsevier.
7. Aboueian-Jahromi, J., A. Hossein Nezhad and A. Behzadmehr, 2011. Effects of inclination angle on the steady flow and heat transfer of power-law fluids around a heated inclined square cylinder in a plane channel, Journal of Non-Newtonian Fluid Mechanics, 166 (23-24): 1406-1414.
8. Datti, P.S., K.V. Prasad, M.S. Abel and A. Joshi, 2004. MHD visco-elastic fluid flow over a non-isothermal stretching sheet, International Journal of Engineering Science, 42(8-9): 935-946.
9. Prasad, K.V., M.S. Abel and S.K. Khan, 2000. Momentum and heat transfer in visco-elastic fluid flow in a porous medium over a non-isothermal stretching sheet, International Journal of Numerical Methods for Heat & Fluid Flow, 10(8): 786-801.
10. Prasad, K.V. and K. Vajravelu, 2009. Heat transfer in the MHD flow of a power law fluid over a non-isothermal stretching sheet, International Journal of Heat and Mass Transfer, 52(21-22): 4956-4965.
11. Abdel-Rahman, G.M., 2013. Effects of variable viscosity and thermal conductivity on unsteady MHD flow of non-Newtonian fluid over a stretching porous sheet, Thermal Science, 17(4): 1035-1047.
12. Raja, M.A.Z. and R. Samar, 2014. Numerical treatment for nonlinear MHD Jeffery-Hamel problem using neural networks optimized with interior point algorithm, Neurocomputing, 124: 178-193.
13. McFall, K.S., 2013. Automated design parameter selection for neural networks solving coupled partial differential equations with discontinuities, Journal of the Franklin Institute-Engineering and Applied Mathematics, 350(2): 300-317.
14. Tsoulos, I.G., D. Gavrilis and E. Glavas, 2009. Solving differential equations with constructed neural networks, Neurocomputing, 72 (10-12): 2385-2391.
15. Choi, B. and J.H. Lee, 2009. Comparison of generalization ability on solving differential equations using backpropagation and reformulated radial basis function networks, Neurocomputing, 73(1-3): 115-118.
16. Islamoglu, Y. and A. Kurt, 2004. Heat transfer analysis using ANNs with experimental data for air flowing in corrugated channels, International Journal of Heat and Mass Transfer, 47(6-7): 1361-1365.
17. Pacheco-Vega, A., M. Sen, K.T. Yang and R.L. McClain, 2001. Neural network analysis of fin-tube refrigerating heat exchanger with limited experimental data, International Journal of Heat and Mass Transfer, 44(4): 763-770.
18. Sreekanth, S., H.S. Ramaswamy, S.S. Sablani and S.O. Prasher, 1999. A neural network approach for evaluation of surface heat transfer coefficient, Journal of Food Processing and Preservation, 23(4): 329-348.
19. Kalogirou, S.A., S. Panteliou and A. Dentsoras, 1999. Artificial neural networks used for the performance prediction of a thermosiphon solar water heater, Renewable Energy, 18(1): 87-99.

20. Sozen, A. and E. Arcaklioglu, 2007. Exergy analysis of an ejector-absorption heat transformer using artificial neural network approach, Applied Thermal Engineering, 27(2-3): 481-491.
21. Gandhidasan, P. and M.A. Mohandes, 2011. Artificial neural network analysis of liquid desiccant dehumidification system, Energy, 36 (2): 1180-1186.
22. Mohammad, A.T., S. Bin Mat, M.Y. Sulaiman, K. Sopian and A.A. Al-abidi, 2013. Artificial neural network analysis of liquid desiccant dehumidifier performance in a solar hybrid air-conditioning system, Applied Thermal Engineering, 59(1-2): 389-397.
23. Rashidi, M.M., M. Ali, N. Freidoonimehr and F. Nazari, 2013. Parametric analysis and optimization of entropy generation in unsteady MHD flow over a stretching rotating disk using artificial neural network and particle swarm optimization algorithm, Energy, 55: 497-510.
24. Neofytou, P., C. Housiadas, S.G. Tsangaris, A.K. Stubos and D.I. Fotiadis, 2013. Newtonian and Power-Law fluid flow in a T-junction of rectangular ducts, Theor. Comput. Fluid Dyn, pp: 1-24.
25. Kasabov, N.K., 1996. Foundations of neural networks, fuzzy systems and knowledge engineering, MIT Press, Cambridge.
26. Haykin, S., 1999. Neural networks : a comprehensive foundation, Prentice-Hall.
27. Freeman, J.A. and D.M. Skapura, 1991. Neural networks : algorithms, applications and programming techniques, Addison-Wesley.
28. Wu, J., G. Zhang, Q. Zhang, J. Zhou and Y. Wang, 2011. Artificial neural network analysis of the performance characteristics of a reversibly used cooling tower under cross flow conditions for heat pump heating system in winter, Energy and Buildings, 43 (7): 1685-1693.